ILC-based tracking control for linear systems with external disturbances via an SMC scheme

Rongni Yang*,† Yingjie Gong,‡ Wojciech Paszke§

20.10.2024

Abstract

Iterative Learning Control (ILC) is renowned for its capability to achieve precise tracking control for systems with repetitive actions at a fixed time interval. However, pursuing the dual objective of high-precision tracking and rapid convergence is a persistent challenge in the field of learning control. To address this problem, a novel ILC method is designed for a class of discrete-time linear systems subject to non-repetitive disturbances in this paper. Particularly, the updating term in ILC is constructed inspired by the principle of sliding mode control (SMC), which results in the learning process being divided into two distinct stages: a rapid reaching stage and a slow sliding stage. As a result, a balance between convergence speed and tracking performance can be ensured via the proposed ILC method. In addition, to attenuate the effects of non-repetitive disturbances, the disturbance compensation mechanism is integrated into the proposed ILC method. Moreover, the optimal value of the learning gain can be determined using the predicted root mean square (RMS) errors of subsequent iterations, eliminating the need for additional tuning actions. Finally, simulation examples are provided to validate the effectiveness and superiority of the proposed new ILC method.

Note to Practitioners— **For many mechanical components in mechatronic systems and robotics, the motions are repeatable. Iterative learning control (ILC) is a well-established technique ideally suited for enhancing the performance of such repetitive tasks without excessive requirements on sensor-feedback quality or control-loop bandwidth. However, most existing ILC approaches in the literature primarily focus on improving convergence accuracy, while little attention is paid to convergence speed in the iteration domain, especially in the presence of disturbances. This paper addresses the limitations of classical ILC schemes, and draws inspiration from the sliding mode control (SMC) technique. To be specific, a novel SMC-based ILC algorithm is proposed that allows to achieve a good balance between**

*This work was supported in part by the National Natural Science Foundation of China under Grant 62273208, and the National Science Centre in Poland under Grant 2023/48/Q/ST7/00205.

†R. Yang is with the School of Control Science and Engineering, Shandong University, Jinan 250061, China (e-mail: rnyang@sdu.edu.cn).

‡Y. Gong is with the School of Control Science and Engineering, Zhejiang University, Hangzhou 310000, China (e-mail: yjgong00@163.com).

§W. Paszke is with the Institute of Automation, Electronic and Electrical Engineering, University of Zielona Góra, ul. Szafrana 2, 65-516 Zielona Góra, Poland (e-mail: w.paszke@iee.uz.zgora.pl).

the fast convergence and precise tracking performance, especially in case of iteration variant disturbances. Also, it will be shown how the optimal learning gains can be determined. Base on the examples of multi-axis gantry robot and injection molding process, simulations support the theoretical results, and meanwhile show the effectiveness and advantage of the proposed ILC strategy.

Iterative learning control (ILC), convergence, sliding mode control (SMC), non-repetitive disturbances.

1 Introduction

Tracking control, a fundamental and significant topic within the control community [35, 10, 20], primarily aims to ensure precise adherence of a considered system to a given reference command [39, 26]. Presently, various advanced control techniques have been employed to achieve accurate tracking control for various dynamical systems [22, 38]. Among these techniques, iterative learning control (ILC) has emerged as one of the most powerful strategies, notably esteemed for its capacity to attain high-precision tracking for systems that iteratively perform repetitive tasks [37, 18]. The fundamental concept behind ILC is to continuously refine the current tracking performance of systems by leveraging information derived from previous iterations, encompassing tracking errors and control inputs [1, 4]. Notably, different from other learning-type methods like adaptive control, focusing on dynamically adjusting control parameters to adapt to environmental changes, the feature of ILC makes it computationally efficient and straightforward to be implemented, requiring less system identification or modeling knowledge. Over the past decades, owing to its straightforward implementation and superior performance, ILC has found successful applications in diverse fields, including chemical processes [28], robotic manufacturing systems [5] and robotic rehabilitation [9].

The performance evaluation of ILC algorithms predominantly hinges on two key metrics: the convergence error over time and the convergence speed across iterations. Various techniques have been developed to enhance the former metric, aiming to reduce tracking errors [11, 31, 23]. For instance, to bolster the robustness of the feedback system and ensure the convergence of the iterative process, a robust ILC scheme was introduced in [27], leveraging Youla parameterization and the μ-synthesis method. Additionally, efforts have been made to further enhance the tracking performance of conventional ILC. In [13], an adaptive robust learning control method was proposed, while in [29], a neural network learning adaptive robust control approach was employed. These methods were respectively utilized to augment the disturbance rejection capability of the considered systems.

Contrary to the considerable focus on enhancing tracking performance through ILC, limited attention has been paid to the convergence speed of ILC, a factor equally critical for performance improvement. In general, convergence rate within the iterative domain is typically quantified by the number of iterations needed to attain the desired system performance. In [14], a gain-scheduled current-cycle ILC approach was introduced for the piezoelectric position stage, showcasing superior tracking performance in both accuracy and convergence speed. Additionally, recent work in [32] addressed the tracking control problem within a finite iteration framework utilizing an ILC scheme.

However, it is important to note that the majority of existing results are established for deterministic systems. Practical applications inevitably involve random noise, including dynamic disturbances and measurement errors [40, 41, 36], which can compromise robustness and decrease convergence rate for uncertain systems [30]. This is primarily due to the fact that a comparatively conservative learning strategy is usually adopted to prioritize tracking performance at the expense of tracking error's convergence.

Literature reviews indicate that some preliminary efforts addressing the above-mentioned issue have been made, such as the utilization of an adaptive gain strategy in [6] and [15]. This approach employs an adaptive gain-based method to mitigate the effects of measurable noise, thereby enhancing transient convergence performance in terms of iterations. More recent advancements have been witnessed in the research conducted in [3, 2], where an enhanced ILC algorithm was investigated for a category of linear uncertain systems. Notably, Armstrong et al. introduced the application of sliding mode control (SMC) to manipulate the error vector in the updating term of ILC, deviating from a sole emphasis on the selection of gain parameters. Moreover, this approach has achieved a trade-off between understanding the system model and achieving convergence speed for systems affected by repetitive disturbances.

It is well-known that SMC is one of the most powerful control techniques to deal with system uncertainties [8], providing robustness against parameter uncertainties and external disturbances. In [19], a robust discrete terminal sliding mode repetitive controller was employed for positioning systems to effectively eliminate the effects of the periodic uncertainties. Similarly, a design strategy to synthesize a modified repetitive SMC was investigated in [17] for a class of discrete-time linear systems subject to periodic exogenous disturbance and plant uncertainties. Actually, SMC has garnered increasing attention due to its simplicity of implementation and rapid response capabilities. However, it is imperative to note that the bound of tracking error is directly associated with the bound of disturbances, potentially leading to tracking errors exceeding acceptable thresholds when disturbances fluctuate significantly. Moreover, the direct extension of existing SMC-based learning control methods to uncertain systems with unknown and non-repetitive disturbances has been deemed infeasible. Consequently, our work aims to address this limitation by incorporating considerations of non-repetitive disturbances to further enhance tracking performance through ILC schemes.

To sum up, the tracking control problem is addressed in this paper for a class of discrete linear time-invariant (LTI) systems subject to non-repetitive disturbances operating repetitively over a finite time interval. Particularly, a novel ILC strategy combined with the SMC technique is proposed and then developed to achieve both a high-precision tracking performance and fast convergence speed. Moreover, a disturbance observer is constructed to obtain the disturbance estimation, thereby achieving a better disturbance rejection. The contributions of this paper are highlighted as follows:

1. A novel ILC law is proposed by integrating the tracking error inspired by the idea of SMC. The resulting learning process can be divided into two steps: a "*fast*" reaching phase and a "*slow*" sliding phase. Then a trade-off between tracking performance and convergence speed can be achieved for the considered system.

2. In contrast to the traditional linear ILC methods which focus on selecting gain parameters, our proposed approach calculates the optimal controller gain using predicted root mean square error from the subsequent iteration, which eliminates the need for manual tuning of gain parameters.

3. Different from the existing work, the developed ILC law incorporates the observer-based disturbance estimation, leading to enhanced disturbance suppression and system robustness.

The rest of this paper is organized as follows. Section 2 presents preliminaries and the problem formulation. Section 3 introduces the modified fast ILC laws for systems with disturbances and provides main paper results on monotonic convergence and design procedures for learning gains. The effectiveness of the proposed scheme is demonstrated in Section 4. Finally, Section 5 concludes the paper.

Notations: $\mathbb{R}$ and $\mathbb{R}^n$ represent the set of real numbers and the n-dimensional Euclidean space, respectively. I_n denotes the identity matrix of size n. The symbol "T" denotes matrix transposition. The Euclidean vector norm is represented by $\|\cdot\|$. The notation diag$\{\cdots\}$ is used to denote a block-diagonal matrix. For a square matrix A, $\rho(A)$ denotes the spectral radius, defined as $\rho(A) = \max_i |\lambda_i(A)|$, where $\lambda_i(A)$ represents the i-th eigenvalue of A. Matrices, unless explicitly stated, are assumed to be compatible for algebraic operations.

2 Problem Formulation

Consider the following discrete-time linear time-invariant (LTI) single-input single-output (SISO) system over a finite time interval $[0, N-1]$:

$$\begin{aligned} x(t+1,k) &= Ax(t,k) + B_u u(t,k) + B_\tau \tau(t,k), \\ y(t,k) &= Cx(t,k), \end{aligned} \tag{1}$$

where $k \geq 0$ is the iteration number, $x(t,k) \in \mathbb{R}^m$, $u(t,k) \in \mathbb{R}$ and $y(t,k) \in \mathbb{R}$ denote the system state, input and output, respectively; $\tau(t,k)$ denotes the non-repetitive disturbances; A, B_u, B_τ and C are known system matrices with appropriate dimensions.

Before proceeding, the following assumptions are given.

Assumption 1 *After each iteration, the system* (1) *resets to the same initial value, i.e.* $x(0,k) = x_0$, $k \geq 0$, *where* x_0 *is a known vector.*

Assumption 2 *The non-repetitive disturbance* $\tau(t,k)$ *(that is* $\tau(t,k-1) \neq \tau(t,k)$*), is assumed to be bounded, that is, there exists a scalar* $a_\tau > 0$ *such that at any time* $t \in [0, N-1]$ *and the* k*th iteration, the following inequality holds*

$$\|\tau(t,k)\| \leq a_\tau.$$

Assumption 3 *The input-output coupling matrix* CB_u *is of full row rank.*

Remark 1 *The main purpose of Assumption 1 is to simplify the following derivations. In fact, the initial state can be any fixed value or randomly varying around a value for all iterations [33, 25].*

Remark 2 *Under Assumption 3, for any given tracking objective* $\boldsymbol{y}_d$ *, there exist an input sequence* $\boldsymbol{u}$ *such that the output tracking error converges.*

Given the desired reference trajectory $y_d(t)$, the tracking error on iteration k is defined as

$$e(t,k) = y_d(t) - y(t,k). \tag{2}$$

As known, a commonly adopted ILC strategy is to construct the current iteration input as that used on the previous iteration plus a correction term, i.e., a control law of the form

$$u(t,k+1) = u(t,k) + \Delta u(t,k), \tag{3}$$

where $\Delta u(t,k)$ indicates the correction term to be designed. Next, if define the following lifted vectors

$$\begin{aligned}
\boldsymbol{u}_k &= [u(0,k)\ u(1,k)\ \cdots u(N-1,k)]^{\mathrm{T}},\\
\boldsymbol{\tau}_k &= [\tau(0,k)\ \tau(1,k)\ \cdots\ \tau(N-1,k)]^{\mathrm{T}},\\
\boldsymbol{y}_k &= [y(1,k)\ y(2,k)\ \cdots\ y(N,k)]^{\mathrm{T}},\\
\boldsymbol{y}_d &= [y(1,d)\ y(2,d)\ \cdots\ y(N,d)]^{\mathrm{T}},\\
\boldsymbol{e}_k &= [e(1,k)\ e(2,k)\ \cdots\ e(N,k)]^{\mathrm{T}}
\end{aligned} \tag{4}$$

then system (1), tracking error (2) and control input (3) can be reformulated as

$$\boldsymbol{y}_k = H\boldsymbol{u}_k + \boldsymbol{\omega}_k, \tag{5}$$

and

$$\begin{aligned}
\boldsymbol{u}_{k+1} &= \boldsymbol{u}_k + \Delta\boldsymbol{u}_k,\\
\boldsymbol{e}_k &= \boldsymbol{y}_d - \boldsymbol{y}_k,
\end{aligned} \tag{6}$$

with $\boldsymbol{\omega}_k = H_0 x_0 + H_\tau \boldsymbol{\tau}_k$,

$$\begin{aligned}
H_0 &= \begin{bmatrix} (CA)^T & (CA^2)^T & \cdots & (CA^N)^T \end{bmatrix}^T,\\
H_\tau &= \begin{bmatrix} CB_\tau & 0 & \cdots & 0\\ CAB_\tau & CB_\tau & \ddots & \vdots\\ \vdots & \ddots & \ddots & 0\\ CA^{N-1}B_\tau & \cdots & CAB_\tau & CB_\tau \end{bmatrix},\\
H &= \begin{bmatrix} CB_u & 0 & \cdots & 0\\ CAB_u & CB_u & \ddots & \vdots\\ \vdots & \ddots & \ddots & 0\\ CA^{N-1}B_u & \cdots & CAB_u & CB_u \end{bmatrix}.
\end{aligned} \tag{7}$$

Consequently, the above representation can facilitate further analysis and control synthesis. Moreover, the design problem can now be formulated. Given system (1), let updating law (3) be applied. The problem addressed in this paper is to select an appropriate $\Delta\boldsymbol{u}_k$ in (3) such that

- the output tracking error converges to zero as $k \to \infty$, and
- better (when comparing alternatives) learning transient behavior is achieved.

3 SMC-based ILC scheme

In the sequel, a version of disturbance observer is constructed and the obtained disturbance estimates are integrated into the learning controller to achieve a better disturbance rejection and tracking performance of the controlled system. Specifically, a disturbance observer based (DOB) ILC algorithm is proposed via SMC technique to achieve a better convergence of the tracking errors in the iteration domain.

3.1 Disturbance observer

Introducing $\boldsymbol{\theta}_k = \boldsymbol{\omega}_k - \boldsymbol{\omega}_{k+1}$ and considering (5) and (6), we have the following equation

$$\boldsymbol{e}_{k+1} = \boldsymbol{e}_k - H\Delta\boldsymbol{u}_k + \boldsymbol{\theta}_k. \tag{8}$$

Also, the below discrete-time disturbance observer [16] is adopted to estimate the actual disturbance,

$$\begin{cases} \widehat{\boldsymbol{\theta}}_k = K\boldsymbol{e}_k - \boldsymbol{z}_k, \\ \boldsymbol{z}_{k+1} = \boldsymbol{z}_k + K(-H\Delta\boldsymbol{u}_k + \widehat{\boldsymbol{\theta}}_k), \end{cases} \tag{9}$$

where $\widehat{\boldsymbol{\theta}}_k = \widehat{\boldsymbol{\omega}}_k - \widehat{\boldsymbol{\omega}}_{k+1}$, $\widehat{\boldsymbol{\omega}}_k$ and $\widehat{\boldsymbol{\theta}}_k$ denote the disturbance estimation and the difference of successive disturbance estimations, respectively. $\boldsymbol{z}_k$ is the observer state. The matrix $K = \text{diag}\{k_1, k_2, \ldots, k_N\}$, where the diagonal elements k_i, $i = 1, \ldots, N$, represent the observer gains and satisfies $|1 - k_i| < 1$.

Remark 3 *Without loss of generality, the initial values of disturbance observer* (9) *are set to be* $\boldsymbol{z}_0 = \boldsymbol{z}_{d0}$, $\widehat{\boldsymbol{\omega}}_0 = \boldsymbol{\omega}_{d0}$, *where* $\boldsymbol{z}_{d0}$ *and* $\boldsymbol{\omega}_{d0}$ *are known vectors. Then it is easy to derive* $\widehat{\boldsymbol{\theta}}_0$ *is bounded, i.e.*

$$\|\widehat{\boldsymbol{\theta}}_0\| \leqslant \|K\|\,\|\boldsymbol{e}_0 - \boldsymbol{z}_{d0}\| \triangleq \kappa. \tag{10}$$

By recalling the definition of $\boldsymbol{\omega}_k$ and Assumption 2, we have $\boldsymbol{\omega}_k$ and $\boldsymbol{\theta}_k$ are bounded, i.e., $\|\boldsymbol{\omega}_k\| \leqslant \beta_W$, $\|\boldsymbol{\theta}_k\| = \|\boldsymbol{\omega}_k - \boldsymbol{\omega}_{k+1}\| \leqslant 2\beta_W$. Further, it derives

$$\|\Delta\boldsymbol{\theta}_k\| = \|\boldsymbol{\theta}_{k+1} - \boldsymbol{\theta}_k\| \leqslant 4\beta_W \triangleq \beta_\theta. \tag{11}$$

Then the following lemma gives the result on the stability of the proposed disturbance observer.

Lemma 1 *Consider the disturbance observer in* (9) *and define the estimation error as* $\tilde{\boldsymbol{\theta}}_k = \boldsymbol{\theta}_k - \widehat{\boldsymbol{\theta}}_k$. *Then, the estimation error is bounded and satisfies*

$$|\tilde{\theta}_k^j| \leq \frac{\beta_\theta}{1 - |\mu_j|}, \tag{12}$$

where $\tilde{\theta}_k^j$ *is the* j*-th element of* $\tilde{\boldsymbol{\theta}}_k$. *Also* $\mu_j = 1 - k_j$, *satisfies* $|\mu_j| < 1$, $j = 1, 2, \ldots, N$.

Proof: The first step is to rewrite (9) as

$$\begin{aligned} \widehat{\boldsymbol{\theta}}_{k+1} &= K\boldsymbol{e}_{k+1} - \boldsymbol{z}_{k+1} \\ &= K(\boldsymbol{e}_k - H\Delta\boldsymbol{u}_k + \boldsymbol{\theta}_k) \\ &\quad -(\boldsymbol{z}_k + K(-H\Delta\boldsymbol{u}_k + \widehat{\boldsymbol{\theta}}_k)) \\ &= K\boldsymbol{e}_k + K\boldsymbol{\theta}_k - \boldsymbol{z}_k - K\widehat{\boldsymbol{\theta}}_k \\ &= \widehat{\boldsymbol{\theta}}_k + K\boldsymbol{\theta}_k - K\widehat{\boldsymbol{\theta}}_k \\ &= (I_N - K)\widehat{\boldsymbol{\theta}}_k + K\boldsymbol{\theta}_k, \end{aligned}$$

which leads to

$$\tilde{\boldsymbol{\theta}}_{k+1} = (I_N - K)\tilde{\boldsymbol{\theta}}_k - \boldsymbol{\theta}_k + \boldsymbol{\theta}_{k+1}.$$

Next, let $\Delta\boldsymbol{\theta}_k^j = \boldsymbol{\theta}_{k+1}^j - \boldsymbol{\theta}_k^j$. Then, we get

$$\begin{aligned}\widetilde{\boldsymbol{\theta}}_{k+1}^j =& \mu_j \widetilde{\boldsymbol{\theta}}_k^j + \Delta\boldsymbol{\theta}_k^j \\ \leq& |\mu_j|^k \left|\widetilde{\boldsymbol{\theta}}_0^j\right| + \sum_{i=0}^{k} |\mu_j|^i \left|\Delta\boldsymbol{\theta}_{k-i-1}^j\right|.\end{aligned}$$

Since $\|\widehat{\boldsymbol{\theta}}_0\| \leqslant \kappa,\ \ \|\Delta\boldsymbol{\theta}_k\| \leqslant \beta_\theta$, one has

$$\begin{aligned}\widetilde{\boldsymbol{\theta}}_{k+1}^j \leq& \kappa |\mu_j|^k + \beta_\theta \sum_{i=0}^{k} |\mu_j|^i \\ \leq& (\kappa - \beta_\theta) |\mu_j|^k + \frac{\beta_\theta}{1 - |\mu_j|}.\end{aligned}$$

Nothing, finally, that $|\mu_j| < 1, j = 1, 2, \ldots, N$, we can conclude that $|\mu_j|^k \to 0$ as $k \to \infty$. Therefore, the disturbance estimation error $\widetilde{\boldsymbol{\theta}}_k^j$ is finally bounded and this completes the proof.

3.2 SMC-based ILC law

In the following, we will focus on the design of an ILC law in the form of (3) by using the concept of SMC. Typically, the design process of SMC involves two stages: constructing a sliding mode surface with satisfactory performance, and designing an appropriate controller to guide the system trajectories from an initial state to the predefined sliding mode surface, ensuring their continuous sliding along the surface until reaching the origin [34, 24, 7]. Meanwhile, inspired by the advantages of SMC technique in terms of robustness against parameter uncertainties and external disturbances, the correction term $\Delta u(t,k)$ in ILC law (3) can be designed as follows:

$$\Delta u(t,k) = \begin{cases} \Delta_1, & |e(t,k)| \geq \rho \\ \Delta_2, & |e(t,k)| < \rho \end{cases} \tag{13}$$

with

$$\begin{aligned}\Delta_1 =& \gamma \tanh\left(|e(t+1,k)|^q\right) \operatorname{sig}^\alpha(e(t+1,k)) \qquad (14)\\ & + l\hat{\theta}(t,k), \quad q = 1 - \alpha, \\ \Delta_2 =& \gamma e(t+1,k) + l\hat{\theta}(t,k), \qquad (15)\end{aligned}$$

where ρ denotes the size of the boundary layer, γ and l are the learning gain and the disturbance compensation gain to be designed later, respectively. Also

$$\operatorname{sig}^\alpha(e(t,k)) = |e(t,k)|^\alpha \operatorname{sgn}(e(t,k)), 0 < \alpha < 1$$

is a continuous non-smooth function.

Remark 4 *It should be noted that in the presented ILC law* (3) *with the updating form* (13), $u(t,k)$ *can be regarded as the current control input, while* Δ_1 *and* Δ_2 *represent the innovation terms. Clearly, information from the* k*-th iteration is utilized to update the* $(k+1)$*-th learning law.*

Specifically, both $x(t,k)$ and $u(t,k)$ are acquired prior to the generation of control input $u(t,k+1)$ at$(k+1)$-th iteration, thereby allowing determination of the corresponding values of $y(t,k)$ and $e(t,k)$. Subsequently, by employing the system equation (1)*, the complete information in lifted form* (4) *can be derived at the k-th iteration, which includes the error signal $e(t+1,k)$.*

Remark 5 *From the correction term* (13) *in ILC law* (3)*, one can see that the learning process is similar to the fast-arrival and slow-slide phases of the SMC method. Particularly, beyond the boundary layer, the updating term* (14) *is employed. Similar to the SMC reaching phase, this phase aims for rapid convergence to the sliding manifold. Once entering the boundary layer, the learning behavior is the same as the traditional ILC law as given in* (15)*, which means that the sliding manifold in this algorithm is a dynamic learning system. Besides, the introduction of disturbance compensation term $l\hat{\theta}(t,k)$ in* (14) *and* (15) *further ensures the system tracking accuracy.*

3.3 Convergence Analysis

Next, the convergence analysis will be conducted in this subsection. The situation that the controlled system enters the slow-slide phase is firstly analyzed. At this point, ILC law with correction (15) is used, while it can be transformed to the lifted framework as follows

$$\boldsymbol{u}_{k+1} = \boldsymbol{u}_k + \Gamma \boldsymbol{e}_k + L\hat{\boldsymbol{\theta}}_k, \tag{16}$$

where $\boldsymbol{e}_k = \boldsymbol{y}_d - \boldsymbol{y}_k$, $\boldsymbol{y}_d = [y_d(1,k)\ y_d(2,k)\ \cdots\ y_d(N,k)]^{\mathrm{T}}$. Γ and L is the constant diagonal matrices whose diagonal elements are γ and l, respectively.

Then, by utilizing the proposed ILC law (3) with correction (15), the sufficient condition of convergence for system (1) with disturbances is given in the following lemma.

Theorem 1 *Assume that an ILC law* (3) *with correction term* (13) *and the disturbance observer* (9) *are applied to the system* (1) *with disturbances. Then the resulting ILC dynamics achieves the convergence of tracking errors if there exists a scalar γ satisfies*

$$0 < \rho(I - \gamma H) < 1. \tag{17}$$

Proof: Substitute the control law in (16) into system (5), and one obtains

$$\begin{aligned}
\boldsymbol{e}_{k+1} =& \boldsymbol{y}_{\boldsymbol{d}} - \boldsymbol{y}_{k+1} \\
=& \boldsymbol{e}_k - \left(\boldsymbol{y}_{k+1} - \boldsymbol{y}_k\right) \\
=& \boldsymbol{e}_k - H\left(\boldsymbol{u}_{k+1} - \boldsymbol{u}_k\right) - \left(\boldsymbol{\omega}_{k+1} - \boldsymbol{\omega}_k\right) \\
=& \boldsymbol{e}_k - H\Gamma \boldsymbol{e}_k - HL\hat{\boldsymbol{\theta}}_k + \boldsymbol{\theta}_k \\
=& (I - H\Gamma)\boldsymbol{e}_k + HL\tilde{\boldsymbol{\theta}}_k + (I - HL)\boldsymbol{\theta}_k.
\end{aligned} \tag{18}$$

Besides, by recalling the results of Lemma 1, we have $\tilde{\boldsymbol{\theta}}_k \leqslant \beta$. Then it can be derived that

$$\limsup_{k\to\infty} \|\boldsymbol{e}_k\| \le \frac{\|HL\|\beta + 2\|I - HL\|\beta_W}{1 - \|I - H\Gamma\|}, \tag{19}$$

which implies the convergence of tracking errors. This completes the proof.

Remark 6 *Considering an ideal scenario with zero disturbance, i.e.,* $\boldsymbol{\theta}_k = 0$*, the iterative dynamics of the tracking error can be derived as* $\boldsymbol{e}_{k+1} = (I - H\Gamma)\boldsymbol{e}_k - HL\hat{\boldsymbol{\theta}}_k$*, showing that tracking performance still relates to the disturbance estimation value. Meanwhile, based on the structure of the proposed disturbance observer, it is evident that as* k *approaches infinity,* $\widehat{\boldsymbol{\theta}}_k$ *converges to zero, ensuring that the tracking error converges to a bounded value. Indeed, the convergence of tracking errors can be always guaranteed regardless of the presence of disturbances under the implementation of the presented disturbance observer. In addition, from* (19)*, it can be seen that the magnitude of the tracking error is directly influenced by the observer gain* L*. Thus, tuning the value of* L *can significantly enhance tracking performance. Consequently, the design of disturbance observers is critical for ensuring robust performance under both ideal and disturbed conditions.*

Next, the learning algorithm outside the boundary layer is addressed. Here, the ILC law has the following form

$$\begin{aligned} u(t, k+1) =& u(t, k) + \gamma \tanh\left(|e(t+1, k)|^q\right) \\ & \operatorname{sig}^\alpha(e(t+1, k)) + l\hat{\theta}(t, k), \end{aligned} \tag{20}$$

and it can be reformulated in the lifted domain as

$$\boldsymbol{u}_{k+1} = \boldsymbol{u}_k + \Gamma \operatorname{Tanh}\left(|\boldsymbol{e}_k|^q\right) \operatorname{Sig}^\alpha(\boldsymbol{e}_k) + L\hat{\boldsymbol{\theta}}_k, \tag{21}$$

where $\operatorname{Sig}^\alpha(\boldsymbol{e}_k) = \operatorname{Ave}^\alpha(\boldsymbol{e}_k)\operatorname{sgn}(\boldsymbol{e}_k)$ with

$$\begin{aligned} \operatorname{Tanh}\left(|\boldsymbol{e}_k|^q\right) =& \operatorname{diag}\{\tanh(|e(0,k)|^q),\ \tanh(|e(1,k)|^q), \\ & \cdots, \tanh(|e(N-1,k)|^q)\}, \\ \operatorname{Ave}(\boldsymbol{e}_k) =& \operatorname{diag}\{|e(0,k)|, |e(1,k)|,\ \cdots, |e(N-1,k)|\}, \\ \operatorname{sgn}(\boldsymbol{e}_k) =& \left[\operatorname{sgn}(e(0,k))\ \ \operatorname{sgn}(e(1,k)) \cdots \operatorname{sgn}(e(N-1,k))\right]^T. \end{aligned}$$

In the following, the reach-ability condition during the fast reaching phase can be derived by utilizing the Lyapunov function technique, which ensures that the tracking error can converge monotonically to the boundary layer.

First, the sliding mode can be designed as $s(k) = \|\boldsymbol{e}_k\|_2$ since the root mean square error is directly related to the scale of boundary layer. Then the following Lyapunov function is constructed

$$V(k) = s^2(k) = \boldsymbol{e}_k^T \boldsymbol{e}_k, \tag{22}$$

and one has

$$\begin{aligned} \Delta V(k) &= V(k+1) - V(k) \\ &= s^2(k+1) - s^2(k) \\ &= \boldsymbol{e}_{k+1}^T \boldsymbol{e}_{k+1} - \boldsymbol{e}_k^T \boldsymbol{e}_k \\ &= 2\boldsymbol{e}_k^T \Delta \boldsymbol{e}_k + \|\Delta \boldsymbol{e}_k\|_2^2, \end{aligned} \tag{23}$$

where

$$\Delta \boldsymbol{e}_k = \boldsymbol{e}_{k+1} - \boldsymbol{e}_k.$$

Also, by combining (5) with (21), it follows that

$$\begin{aligned}\Delta \boldsymbol{e}_k =& -\left(\boldsymbol{y}_{k+1}-\boldsymbol{y}_k\right)\\ =& -H\left(\boldsymbol{u}_{k+1}-\boldsymbol{u}_k\right)-\left(\boldsymbol{\omega}_{k+1}-\boldsymbol{\omega}_k\right)\\ =& -H\Gamma\,\mathrm{Tanh}\left(|\boldsymbol{e}_k|^q\right)\mathrm{Sig}^\alpha(\boldsymbol{e}_k)-HL\hat{\theta}(k)\\ &+\boldsymbol{\theta}_k\\ =& -H\Gamma\,\mathrm{Tanh}\left(|\boldsymbol{e}_k|^q\right)\mathrm{Sig}^\alpha(\boldsymbol{e}_k)+HL\tilde{\boldsymbol{\theta}}_k\\ &+(I-HL)\boldsymbol{\theta}_k.\end{aligned} \tag{24}$$

By substituting (24) into (23), we have

$$\begin{aligned}\Delta V(k) =& -2\boldsymbol{e}_k^T[H\Gamma\,\mathrm{Tanh}\left(|\boldsymbol{e}_k|^q\right)\mathrm{Sig}^\alpha(\boldsymbol{e}_k)-HL\tilde{\boldsymbol{\theta}}_k\\ &-(I-HL)\boldsymbol{\theta}_k]+\|H\Gamma\,\mathrm{Tanh}\left(|\boldsymbol{e}_k|^q\right)\mathrm{Sig}^\alpha(\boldsymbol{e}_k)\\ &-HL\tilde{\boldsymbol{\theta}}_k-(I-HL)\boldsymbol{\theta}_k\|_2^2.\end{aligned} \tag{25}$$

Note that the tracking errors of the system is convergent if $\Delta V(k) < 0$. That is, the system can be driven toward the boundary layer monotonically until the condition is not feasible and the system enters into the slow-sliding phase.

Remark 7 *Based on the above discussion, the switching between fast reaching phase with ILC law* (21) *and slow sliding phase with ILC law* (16) *is determined by the Lyapunov difference function* $\Delta V(k)$. *Correspondingly, if* $\Delta V(k) < 0$, *the system will enter fast reaching phase and remains stable. Otherwise, if* $\Delta V(k) > 0$, *the system will switch to slow sliding phase. Therefore, rather than setting a constant* ρ, *the boundary layer can be selected as* $\Delta V(k)$. *In this way, there is no need to tune the parameters.*

Thus, we are now in a position to state the following result.

Theorem 2 *Assume that an ILC law* (3) *with correction term* (13) *is applied to the system* (1). *Then the resulting ILC dynamics achieves the convergence of tracking errors if there exist a scalar* γ *such that*

1. *the condition* (17) *in Lemma 1 holds,*
2. $\gamma_{max} < \frac{\|\boldsymbol{e}_0\|_2}{\|m\|_2}$, *where* $m = H\,\mathrm{Tanh}\left(|\boldsymbol{e}_0|^q\right)\mathrm{Sig}^\alpha(\boldsymbol{e}_0)$.

Proof: From the previous analysis, the convergence of tracking errors for the system (1) can be achieved if $\Delta V(k) < 0$. Besides, the system should be ensured to enter the fast reaching phase and remain stable before switching to the slow sliding phase. To this end, the following inequality must hold,

$$\Delta V(0) < 0. \tag{26}$$

Then one has

$$\begin{aligned}\Delta V(0) &= -2\gamma\boldsymbol{e}_0^T[H\,\mathrm{Tanh}\left(|\boldsymbol{e}_0|^q\right)\mathrm{Sig}^\alpha(\boldsymbol{e}_0)\\ &\quad -HL\tilde{\boldsymbol{\theta}}_0-(I-HL)\boldsymbol{\theta}_0]\\ &\quad +\|\gamma H\,\mathrm{Tanh}\left(|\boldsymbol{e}_0|^q\right)\mathrm{Sig}^\alpha(\boldsymbol{e}_0)-HL\tilde{\boldsymbol{\theta}}_0\\ &\quad -(I-HL)\boldsymbol{\theta}_0\|_2^2\\ &= m^Tm\gamma^2-2n^Tm\gamma+n^Tn-\boldsymbol{\theta}_0^T\boldsymbol{e}_0\\ &= \|m\gamma-n\|_2^2-\|\boldsymbol{e}_0\|_2^2,\end{aligned} \tag{27}$$

with

$$\begin{aligned} m &= H\,\mathrm{Tanh}\left(|\boldsymbol{e}_0|^q\right)\mathrm{Sig}^{\alpha}(\boldsymbol{e}_0), \\ n &= \boldsymbol{e}_0 + HL\tilde{\boldsymbol{\theta}}_0 + (I - HL)\boldsymbol{\theta}_0. \end{aligned}$$

Note that the data from the first iteration are used in the calculation of $\Delta V(0)$. The iteration $k = 0$ represents the initial run and the learning control has not been applied yet. This implies that the inequality (26) is solved in an off-line manner. Apparently, it follows from (26)-(27) that

$$\|m\gamma - n\|_2^2 < \|\boldsymbol{e}_0\|_2^2 \,. \tag{28}$$

Furthermore, it should be noted that the parameter n encompasses the disturbance variable, making it impossible to directly derive the range of γ from equation (28). Consequently, we employ the following norm scaling technique to address this, resulting in

$$\|m\gamma - n\|_2^2 \le \left(\|m\gamma\|_2 + \|n\|_2\right)^2 < \|\boldsymbol{e}_0\|_2^2 \,, \tag{29}$$

which directly leads to

$$\|m\gamma\|_2 \;\;<\;\; \|\boldsymbol{e}_0\|_2 - \|n\|_2 \,. \tag{30}$$

After some simple calculations, we obtain

$$\gamma < \frac{\|\boldsymbol{e}_0\|_2}{\|m\|_2}. \tag{31}$$

Thus, if the controller gain γ satisfies (31), the system in (1) under ILC law of (3) and (13) can enter fast reaching phase and the asymptotic convergence of tracking errors is also achieved. Meanwhile, if $\Delta V(k) > 0$, the ILC law switches to (16). Then based on Theorem 1, the considered system is still stable.

In conclusion, based the above analysis, the convergence of tracking errors for system (1) under the iterative learning controller (3) with updating law (13) has been achieved. This completes the proof. It should be noted that although the bound of gain γ is provided in Theorem 2 when the system (1) is within the fast reaching phase, an explicit way to calculate the gain parameters γ and l is not provided yet. In the following, the method to obtain the gain parameters will be explored. As the result, the proposed ILC scheme, where the gain parameters are calculated with the provided design procedure, gives the significant improvement of tracking errors.

Theorem 3 *Assume that an ILC law* (3) *with correction term* (13) *is applied to the system* (1)*. Then the resulting ILC dynamics achieves the convergence of tracking errors. Moreover, the optimal values of gain γ and l in the proposed learning controller can be calculated by*

$$\gamma^* = \frac{\Pi_1}{\Pi}, \quad l^* = \frac{\Pi_2}{\Pi}, \tag{32}$$

where

$$\begin{aligned} &\Pi_1 = \begin{vmatrix} \boldsymbol{a}^T\boldsymbol{b} & \boldsymbol{b}^T\boldsymbol{b} \\ \boldsymbol{a}^T\boldsymbol{c} & \boldsymbol{c}^T\boldsymbol{b} \end{vmatrix}, \; \Pi_2 = \begin{vmatrix} \boldsymbol{a}^T\boldsymbol{b} & \boldsymbol{a}^T\boldsymbol{a} \\ \boldsymbol{c}^T\boldsymbol{b} & \boldsymbol{a}^T\boldsymbol{c} \end{vmatrix}, \; \Pi = \begin{vmatrix} \boldsymbol{a}^T\boldsymbol{a} & \boldsymbol{a}^T\boldsymbol{b} \\ \boldsymbol{a}^T\boldsymbol{b} & \boldsymbol{b}^T\boldsymbol{b} \end{vmatrix} \\ &\boldsymbol{a} = -\,H\,\mathrm{Tanh}\left(|\boldsymbol{e}_0|^q\right)\mathrm{Sig}^{\alpha}(\boldsymbol{e}_0), \;\; \boldsymbol{b} = H\hat{\boldsymbol{\theta}}_0, \\ &\boldsymbol{c} = \hat{\boldsymbol{e}}_{\mathbf{0}} + \hat{\boldsymbol{\theta}}_0. \end{aligned}$$

As a result, a significant improvement of tracking errors can be achieved by using the proposed ILC scheme with the optimal parameters above.

Proof: First, the largest rms error improvement between iterations $k = 0$ and $k = 1$ is considered, which means how to minimize the predicted RMS error of iteration $k = 1$. From (24), it can be given that

$$\begin{aligned} \boldsymbol{e}_1 =& \boldsymbol{e}_0 - \gamma H \operatorname{Tanh}(|\boldsymbol{e}_0|^q) \operatorname{Sig}^\alpha(\boldsymbol{e}_0) \\ & - HL\tilde{\boldsymbol{\theta}}_0 - (I - HL)\boldsymbol{\theta}_0. \end{aligned} \tag{33}$$

Due to the existence of non-repetitive disturbance, the predicted error of iteration $k = 1$ shown in (33) is not available. To solve this problem, the prediction of error is adopted. Then we have

$$\begin{aligned} \hat{\boldsymbol{e}}_{\boldsymbol{1}} &= \boldsymbol{y_d} - \hat{\boldsymbol{y}}_1 \\ &= \hat{\boldsymbol{e}}_{\boldsymbol{0}} + \hat{\boldsymbol{y}}_0 - \hat{\boldsymbol{y}}_1 \\ &= \hat{\boldsymbol{e}}_{\boldsymbol{0}} - H\Delta \boldsymbol{u}_0 + \hat{\boldsymbol{\theta}}_0 \\ &= \hat{\boldsymbol{e}}_{\boldsymbol{0}} - H[\Gamma \operatorname{Tanh}(|\boldsymbol{e}_0|^q) \operatorname{Sig}^\alpha(\boldsymbol{e}_0) + L\hat{\boldsymbol{\theta}}_0] + \hat{\boldsymbol{\theta}}_0 \\ &= \hat{\boldsymbol{e}}_{\boldsymbol{0}} - \gamma H \operatorname{Tanh}(|\boldsymbol{e}_0|^q) \operatorname{Sig}^\alpha(\boldsymbol{e}_0) \\ &\quad + (I - HL)\hat{\boldsymbol{\theta}}_0. \end{aligned} \tag{34}$$

Meanwhile, based on the disturbance observer (9), it can be derived that

$$\hat{\boldsymbol{\theta}}_0 = K\boldsymbol{e}_0 - \boldsymbol{z}_0. \tag{35}$$

Furthermore, the predicted rms error on iteration $k = 1$ is

$$\|\boldsymbol{e}_1\|_2 = \sqrt{\Phi^T \Phi}, \tag{36}$$

where

$$\Phi = \hat{\boldsymbol{e}}_{\boldsymbol{0}} - \gamma H \operatorname{Tanh}(|\boldsymbol{e}_0|^q) \operatorname{Sig}^\alpha(\boldsymbol{e}_0) + (I - lH)\hat{\boldsymbol{\theta}}_0.$$

Apparently, obtaining the minimum of $\|\boldsymbol{e}_1\|_2$ is equivalent to minimize $\|\boldsymbol{e}_1\|_2^2$. Next, for simplifying the derivation, some notations are introduced as follows:

$$\begin{aligned} \boldsymbol{a} &= -H \operatorname{Tanh}(|\boldsymbol{e}_0|^q) \operatorname{Sig}^\alpha(\boldsymbol{e}_0), \\ \boldsymbol{b} &= H\hat{\boldsymbol{\theta}}_0, \\ \boldsymbol{c} &= \hat{\boldsymbol{e}}_{\boldsymbol{0}} + \hat{\boldsymbol{\theta}}_0. \end{aligned}$$

Then the optimization problem can be reformulated as

$$\text{Objective: } \min J(\gamma, l) = \|\boldsymbol{e}_1\|_2^2 = \Phi^T \Phi, \tag{37}$$

where

$$\Phi = \gamma \boldsymbol{a} + l\boldsymbol{b} + \boldsymbol{c}.$$

The derivative of objective function in (37) is first calculated, while making the resulted function equal to zero. So it can be derived that

$$\begin{cases} \frac{\partial J}{\partial \gamma} = 2\boldsymbol{a}^T\boldsymbol{a}\gamma + 2\boldsymbol{a}^T\boldsymbol{b}l + 2\boldsymbol{a}^T\boldsymbol{c} = 0, \\ \frac{\partial J}{\partial l} = 2\boldsymbol{a}^T\boldsymbol{b}\gamma + 2\boldsymbol{b}^T\boldsymbol{b}l + 2\boldsymbol{c}^T\boldsymbol{b} = 0, \end{cases} \tag{38}$$

which is equivalent to

$$\begin{bmatrix} \boldsymbol{a}^T\boldsymbol{a} & \boldsymbol{a}^T\boldsymbol{b} \\ \boldsymbol{a}^T\boldsymbol{b} & \boldsymbol{b}^T\boldsymbol{b} \end{bmatrix} \begin{bmatrix} \gamma \\ l \end{bmatrix} = \begin{bmatrix} -\boldsymbol{a}^T\boldsymbol{c} \\ -\boldsymbol{c}^T\boldsymbol{b} \end{bmatrix}. \tag{39}$$

Because the following inequality holds when $\boldsymbol{a} \neq \boldsymbol{b}$,

$$\begin{aligned} \Pi = & \begin{vmatrix} \boldsymbol{a}^T\boldsymbol{a} & \boldsymbol{a}^T\boldsymbol{b} \\ \boldsymbol{a}^T\boldsymbol{b} & \boldsymbol{b}^T\boldsymbol{b} \end{vmatrix} \\ = & \boldsymbol{a}^T\boldsymbol{a} \cdot \boldsymbol{b}^T\boldsymbol{b} - \boldsymbol{a}^T\boldsymbol{b} \cdot \boldsymbol{a}^T\boldsymbol{b} \neq 0. \end{aligned} \tag{40}$$

Thus, the equation set of (39) has a unique solution. By straightforward calculation, we have

$$\begin{aligned} \begin{bmatrix} \gamma^* \\ l^* \end{bmatrix} = & \begin{bmatrix} \boldsymbol{a}^T\boldsymbol{a} & \boldsymbol{a}^T\boldsymbol{b} \\ \boldsymbol{a}^T\boldsymbol{b} & \boldsymbol{b}^T\boldsymbol{b} \end{bmatrix}^{-1} \begin{bmatrix} -\boldsymbol{a}^T\boldsymbol{c} \\ -\boldsymbol{c}^T\boldsymbol{b} \end{bmatrix} \\ = & -\frac{1}{\Pi} \begin{bmatrix} \boldsymbol{b}^T\boldsymbol{b} \cdot \boldsymbol{a}^T\boldsymbol{c} - \boldsymbol{a}^T\boldsymbol{b} \cdot \boldsymbol{c}^T\boldsymbol{b} \\ -\boldsymbol{a}^T\boldsymbol{b} \cdot \boldsymbol{a}^T\boldsymbol{c} + \boldsymbol{a}^T\boldsymbol{a} \cdot \boldsymbol{c}^T\boldsymbol{b} \end{bmatrix}. \end{aligned}$$

Further, (γ^*, l^*) can be obtained in (32), which is also known as the stationary point of the equation set in (38). Then we will prove that (γ^*, l^*) is the minimum point of the objective function (37). To this end, the second partial derivative of (37) is taken, and we have

$$\begin{aligned} J_{\gamma\gamma} = & \frac{\partial^2 J}{\partial \gamma^2} = 2\boldsymbol{a}^T\boldsymbol{a}, \\ J_{\gamma l} = & J_{\gamma l}^T = \frac{\partial}{\partial l}(\frac{\partial J}{\partial \gamma}) = 2\boldsymbol{a}^T\boldsymbol{b}, \\ J_{ll} = & \frac{\partial^2 J}{\partial l^2} = 2\boldsymbol{b}^T\boldsymbol{b}. \end{aligned}$$

Moreover, we have

$$\begin{aligned} J_{\gamma l}^2 - J_{\gamma\gamma}J_{ll} = & 4(\boldsymbol{a}^T\boldsymbol{b}) \cdot (\boldsymbol{a}^T\boldsymbol{b}) - 4(\boldsymbol{a}^T\boldsymbol{a}) \cdot (\boldsymbol{b}^T\boldsymbol{b}) \\ = & 4[(\boldsymbol{a}^T\boldsymbol{b}) \cdot (\boldsymbol{a}^T\boldsymbol{b}) - (\boldsymbol{a}^T\boldsymbol{a}) \cdot (\boldsymbol{b}^T\boldsymbol{b})]. \end{aligned}$$

According to the Cauchy-Schwarz inequality, it can be derived that

$$J_{\gamma l}^2 - J_{\gamma\gamma}J_{ll} < 0. \tag{41}$$

Therefore, based on $J_{\gamma\gamma} > 0$ and (41), it can be concluded that (γ^*, l^*) is the minimum point of (37). This completes the proof.

4 Illustrate Example

In this section two numerical examples are provided to illustrate the effectiveness, robustness, and advantages of the new results in this paper.

4.1 Example 1: Multi-axis gantry robot

First, an example of multi-axis gantry robot is used [21]. It is important to note that the robot is Cartesian, which implies that the axes are dynamically decoupled and can be considered separately. For the purpose of illustrating the superiority of the ILC algorithm, we focus on the state-space model of the X-axis, which can be expressed as follows:

$$\begin{aligned} x(t+1,k) &= Ax(t,k) + B_u u(t,k) + B_\tau \tau(t,k), \\ y(t,k) &= Cx(t,k), \end{aligned} \tag{42}$$

with

$$A = \begin{bmatrix} 2.41 & -0.86 & 0.85 & -0.59 & 0.30 & -0.19 & 0.32 \\ 4.00 & 0 & 0 & 0 & 0 & 0 & 0 \\ 0 & 1.00 & 0 & 0 & 0 & 0 & 0 \\ 0 & 0 & 1.00 & 0 & 0 & 0 & 0 \\ 0 & 0 & 0 & 1.00 & 0 & 0 & 0 \\ 0 & 0 & 0 & 0 & 0.50 & 0 & 0 \\ 0 & 0 & 0 & 0 & 0 & 0.25 & 0 \end{bmatrix},$$

$$B_u = \begin{bmatrix} 0.0313 \\ 0 \\ 0 \\ 0 \\ 0 \\ 0 \\ 0 \end{bmatrix}, \ B_\tau = \begin{bmatrix} 1 \\ 1 \\ 1 \\ 1 \\ 1 \\ 1 \\ 1 \end{bmatrix}, \ C^T = \begin{bmatrix} 0.0095 \\ -0.0023 \\ 0.0048 \\ -0.0027 \\ 0.0029 \\ -0.0011 \\ 0.0029 \end{bmatrix}.$$

Without loss of generality, the initial operating conditions are as follows:

$$x(0,k) = 0, \ u(t,0) = 0, \forall k \in \mathbb{N}, t \in [0, 10].$$

Also, the desired reference trajectory is set to be $y_d(t) = 0.06\sin(2t - \pi/3)$. Besides, the Root Mean Square (RMS) value of the tracking error defined by

$$\mathrm{RMS}(e_k) = \sqrt{\frac{1}{11}\sum_{t=1}^{11} e^2(t,k)}$$

is adopted as a performance index to evaluate the tracking performance.

In simulations, two control strategies are also considered for comparisons: one is the traditional linear iterative learning controller (LILC), such as a P-type ILC law with the following form

$$LILC: \quad u(t,k+1) = u(t,k) + k_1 e(t+1,k),$$

the other is the fast learning controller proposed in [3].

4.1.1 Simulation Results with Nominal Model

In order to illustrate the effectiveness of the proposed method, the model without disturbance is analysed firstly. Based on the results of Theorem 3, the controller gain can be obtained as:

$\gamma_{opt} = 511.78$, Note that the same selection of gain parameter is adopted in the phase of linear ILC implementation.

Now the controlled dynamic is simulated over 500 iterations. The evolution of tracking errors of considered methods are shown in Fig. 1. It can be seen that both tracking errors under the different ILC control schemes converge to 0 as k converges to infinity. Furthermore, the proposed method converges much faster than the other two methods in the initial phase, which is of great practical importance as it implies potentially significant time/cost savings. Fig. 2 displays the reference trajectories (represented by black dashed lines) and the real trajectories at the kth iteration (with $k = 2, 20, 100, 200$). These trajectories are obtained under various ILC schemes, with the proposed method depicted in red, the method outlined in [3] in blue, and the LILC scheme in green, as indicated by the solid lines. It is clear that the output trajectory can effectively track the reference trajectory as the number of iterations increases.

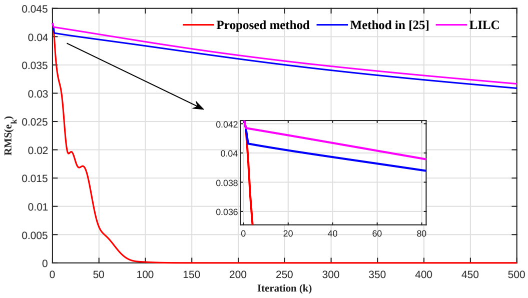

Figure 1: RMS values of tracking errors.

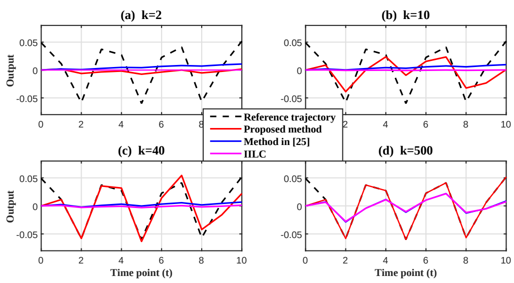

Figure 2: The output trajectories without disturbance.

4.1.2 Simulation Results with iteration-varying disturbance

The non-repetitive disturbances are taken to be

$$\tau(t, k) = \sin(0.05\pi t) + 2\delta_v(t, k) + 0.5\cos(0.02\pi k),$$

where δ_v denote iteration-varying uncertainties, each element of which varies arbitrarily in the interval $[-0.05, 0.05]$. Then it can be verified that Assumptions 1 is guaranteed.

First, the disturbance observer in (9) is adopted, and the observer gain is selected as $K = 0.2 \otimes I_{nN}$. Fig. 3 gives the error of the difference in the estimation of successive disturbance over the first 100 iterations, which implies the convergence of the disturbance observer. Accordingly, the feasibility for subsequent trajectory compensation are guaranteed.

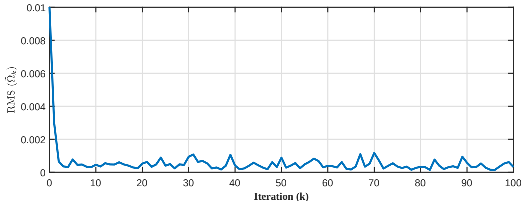

Figure 3: The RMS errors of the disturbance estimation.

Then according to Theorem 3, it can be obtained that

$$\gamma_{opt} = 198.87 \ , \qquad l_{opt} = -1435.87 \ .$$

The simulation results are presented in Figs. 4–6. The tracking error by using different ILC scheme are depicted in Fig. 4. It is obvious that both the utilized method in [3] and the LILC method generate large fluctuations after a few iterations.

In contrast, by using the compensation based on the disturbance observer, the proposed control scheme can effectively attenuate the disturbance, thereby showing better tracking performance. Fig. 5 presents the output trajectories without disturbance at the kth ($k = 5, 50, 200, 500$) iteration under different ILC schemes. Obviously, when the number of iterations reaches 200, the proposed controller can achieve a more accurate tracking compared with the other two methods. In other words, it indicates that the proposed ILC scheme can still ensure a better convergence and tracking performance in the presence of non-repetitive disturbance in contrast to the other ILC algorithms. In addition, in order to further illustrate the superiority of the designed control law, the ILC updating law with/without DOB is compared in Fig. 6, which implies that the use of DOB can also enhance the tracking performance.

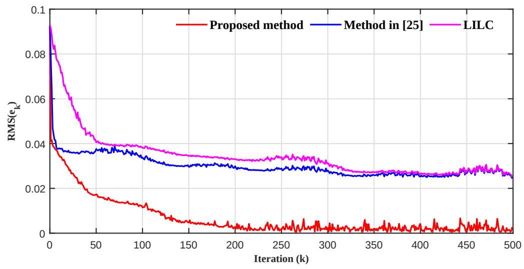

Figure 4: RMS values of tracking errors with disturbances.

4.2 Example 2: Injection molding process

To further substantiate the efficacy of the proposed approach, other examination is conducted on an injection molding process [12]. This procedure encompasses three primary phases: filling, packing/holding, and cooling. In the context of the packing stage, a pivotal process parameter under

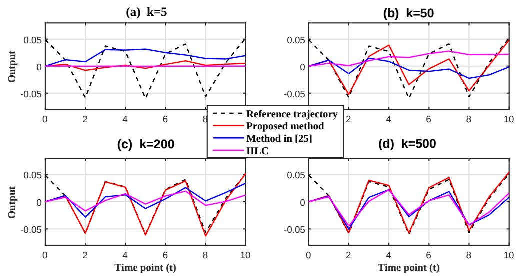

Figure 5: The output trajectories with disturbance.

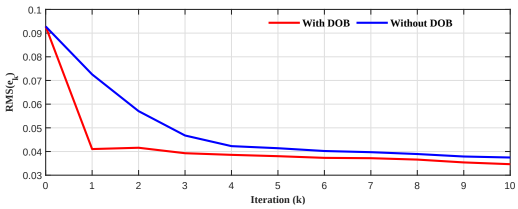

Figure 6: RMS values of tracking errors.

consideration is the nozzle pressure. Utilizing data from open-loop experiments, a mathematical model characterizing the relationship between the nozzle pressure and the hydraulic control valve opening was successfully determined as follows:

$$
\begin{aligned}
x(t+1,k) &= \begin{bmatrix} 1.607 & 1 \\ -0.6086 & 0 \end{bmatrix} x(t,k) + \begin{bmatrix} 1.239 \\ -0.9282 \end{bmatrix} u(t,k) \\
&\quad + \begin{bmatrix} 1 \\ 0 \end{bmatrix} w(t,k), \\
y_k(t) &= \begin{bmatrix} 1 & 0 \end{bmatrix} x_k(t).
\end{aligned}
$$

where the disturbance $w(t,k)$ is chosen as: $w(t,k) = 5\sin(\upsilon_1 0.1t + \upsilon_2 0.2k)$, with υ_1 and υ_2 varying arbitrarily in the interval $[0,1]$. Moreover, the desired reference trajectory is taken as

$$
y_d(t) = \begin{cases} 200, & 0 \le t \le 100 \\ 200 + 5(t-100), & 100 < t \le 120 \\ 300, & 120 < t \le 200 \end{cases}
$$

Building on the results derived from the proposed Theorem 3, when the system is free from disturbances, the controller gain can be calculated as $\gamma_{opt} = 0.0201$. However, when disturbances are present, the controller gain can be determined as follows:

$$
\gamma_{opt} = 0.0188, \quad l_{opt} = -0.0027.
$$

To illustrate the convergence behavior of the introduced methodology and contrast it with existing approaches, Fig. 7 displays the RMS values of tracking errors. It is noteworthy that the proposed method exhibits rapid convergence, regardless of the presence of disturbances. Notably, during the initial fast-reaching phase, it ensures a monotonically decreasing convergence of tracking errors, whereas the conventional linear ILC scheme only attains asymptotic convergence. Figs. 8–9 present the actual output profiles in both disturbed and undisturbed scenarios at the 2nd, 20th, 50th, and 100th iterations, alongside the desired reference trajectory (the black dotted line). Evidently, the tracking performance becomes satisfactory after a small number of iterations. The fluctuations in the output profiles can be attributed to non-repetitive disturbances inherent in the system. The convergence of the actual output profiles with the desired output profile serves as compelling evidence for the effectiveness of the proposed approach.

Additionally, to further elucidate the universality of the presented control scheme, Fig. 10 depicts the RMS values of tracking errors with varying initial values. It is evident that while the configuration of the designed parameters γ_{opt} and l_{opt} is influenced by the initial value of tracking errors, it is noteworthy that the proposed method consistently exhibits a rapid convergence. Moreover, as depicted in Fig. 10, a higher initial RMS value of the tracking error corresponds to a superior final convergence accuracy. For instance, when the initial value is $x_0 = 60$, resulting in the largest initial error e_0, the final error is minimized; Conversely, when the initial value is $x_0 = -60$, resulting in the smallest initial error e_0, the final error is maximized.

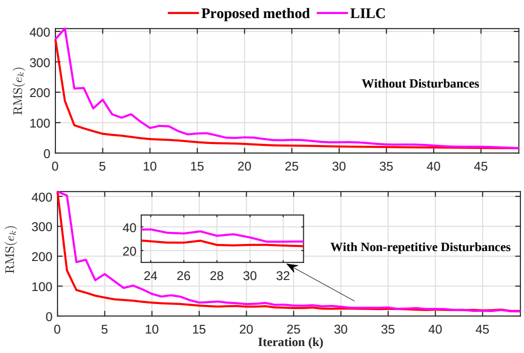

Figure 7: RMS values of tracking errors.

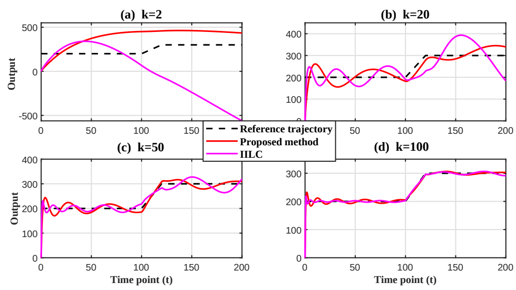

Figure 8: The output trajectories without disturbance.

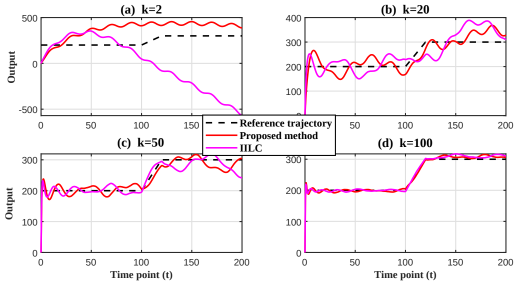

Figure 9: The output trajectories with disturbance.

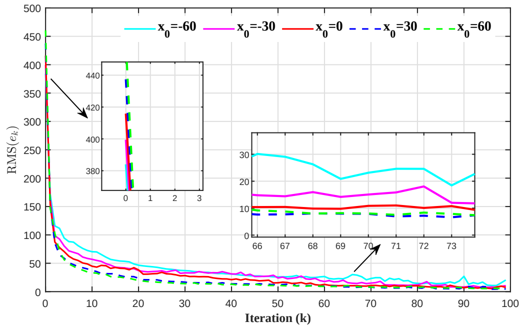

Figure 10: RMS values of tracking errors with different initial values.

5 Conclusion

This paper addresses the tracking control problem by using ILC approach for discrete-time linear SISO systems subject to non-repetitive disturbances. A novel fast ILC scheme, combined with a disturbance observer, is proposed by integrating the principles of SMC. Sufficient conditions for achieving monotonic convergence of the tracking errors are provided. Moreover, the optimal values of the learning gain and the disturbance gain are determined by using information obtained from the initial iterations, ensuring maximum improvement of the learning scheme with respect to tracking error. Finally, the effectiveness of the proposed fast ILC method is validated through a simulation example. Future work aims at extending the proposed ILC laws to nonlinear systems with input and output constraints.

References

[1] Hyo-Sung Ahn, YangQuan Chen, and Kevin L Moore. Iterative learning control: Brief survey and categorization. *IEEE Transactions on Systems, Man, and Cybernetics, Part C (Applications and Reviews)*, 37(6):1099–1121, 2007.

[2] Ashley A Armstrong and Andrew G Alleyne. An improved iterative learning control for uncertain multi-axis systems. In *2020 American Control Conference (ACC)*, pages 4810–4816, 2020.

[3] Ashley A Armstrong, Amy J Wagoner Johnson, and Andrew G Alleyne. An improved approach to iterative learning control for uncertain systems. *IEEE Transactions on Control Systems Technology*, 29(2):546–555, 2021.

[4] Douglas A Bristow, Marina Tharayil, and Andrew G Alleyne. A survey of iterative learning control. *IEEE control systems magazine*, 26(3):96–114, 2006.

[5] Yiyang Chen and Christopher T. Freeman. Iterative learning control for piecewise arc path tracking with validation on a gantry robot manufacturing platform. *ISA Transactions*, 139:650–659, 2023.

[6] Xiang Cheng, Hao Jiang, Dong Shen, and Xinghuo Yu. A novel adaptive gain strategy for stochastic learning control. *IEEE Transactions on Cybernetics*, 53(8):5264–5275, 2022.

[7] Wenhui Dou, Shihong Ding, and Xinghuo Yu. Event-triggered second-order sliding-mode control of uncertain nonlinear systems. *IEEE Transactions on Systems, Man, and Cybernetics: Systems*, 53(11):7269–7279, 2023.

[8] Haibo Du, Xinghuo Yu, Michael ZQ Chen, and Shihua Li. Chattering-free discrete-time sliding mode control. *Automatica*, 68:87–91, 2016.

[9] Chris T. Freeman, A.-M Hughes, J. H. Burridge, P. H. Chappell, P. L. Lewin, and E. Rogers. Iterative learning control of FES applied to the upper extremity for rehabilitation. *Control Engineering Practice*, 17(3):368–381, 2009.

[10] Lan Gao, Hao Lu, Jianliang Wang, Xiang Yu, Peng Jiang, Fei Chen, and Huaqing Li. Robust distributed average tracking with disturbance observer control. *IEEE Transactions on Automation Science and Engineering*, pages 1–14, 2024. DOI:10.1109/TASE.2024.3357527.

[11] Shoulin Hao, Tao Liu, Wojciech Paszke, and Krzysztof Galkowski. Robust iterative learning control for batch processes with input delay subject to time-varying uncertainties. *IET Control Theory & Applications*, 10(15):1904–1915, 2016.

[12] Shoulin Hao, Tao Liu, Wojciech Paszke, Krzysztof Gałkowski, and Qing-Guo Wang. Robust static output feedback based iterative learning control design with a finite-frequency-range two-dimensional specification for batch processes subject to nonrepetitive disturbances. *International Journal of Robust and Nonlinear Control*, 31(12):5745–5761, 2021.

[13] Chuxiong Hu, Ze Wang, Yu Zhu, Ming Zhang, and Hao Liu. Performance-oriented precision larc tracking motion control of a magnetically levitated planar motor with comparative experiments. *IEEE Transactions on Industrial Electronics*, 63(9):5763–5773, 2016.

[14] Deqing Huang, Jian-Xin Xu, Venkatakrishnan Venkataramanan, and The Cat Tuong Huynh. High-performance tracking of piezoelectric positioning stage using current-cycle iterative learning control with gain scheduling. *IEEE Transactions on Industrial Electronics*, 61(2):1085–1098, 2013.

[15] Hao Jiang, Dong Shen, Shunhao Huang, and Xinghuo Yu. Accelerated learning control for point-to-point tracking systems. *IEEE Transactions on Neural Networks and Learning Systems*, 35(1):1265–1277, 2024.

[16] Kyung-Soo Kim and Keun-Ho Rew. Reduced order disturbance observer for discrete-time linear systems. *Automatica*, 49(4):968–975, 2013.

[17] Edi Kurniawan, Hai Wang, Bernadus H Sirenden, Jalu A Prakosa, Hendra Adinanta, and Suryadi Suryadi. Discrete-time modified repetitive sliding mode control for uncertain linear systems. *International Journal of Adaptive Control and Signal Processing*, 35(11):2245–2258, 2021.

[18] Zijian Luo, Wenjun Xiong, Wangli He, and Yao Chen. Observer-based state tracking for discrete linear multi-agent systems with switching topologies via learning control strategies. *IET Control Theory & Applications*, 14(12):1639–1647, 2020.

[19] M Mitrevska, Z Cao, J Zheng, E Kurniawan, and Z Man. Discrete terminal sliding mode repetitive control for a linear actuator with nonlinear friction and uncertainties. *International Journal of Robust and Nonlinear Control*, 29(13):4285–4297, 2019.

[20] Tong Mu, Zhong-Hua Pang, Haibin Guo, Guo-Ping Liu, and Qing-Long Han. Output tracking predictive control of uncertain networked control systems. *IEEE Transactions on Circuits and Systems II: Express Briefs*, 71(6):3141–3145, 2024.

[21] James D Ratcliffe, Paul L Lewin, Eric Rogers, Jari J Hatonen, and David H Owens. Norm-optimal iterative learning control applied to gantry robots for automation applications. *IEEE Transactions on Robotics*, 22(6):1303–1307, 2006.

[22] Wei Ren and Junlin Xiong. Tracking control of nonlinear networked and quantized control systems with communication delays. *IEEE Transactions on Automatic Control*, 65(8):3685–3692, 2019.

[23] Eric Rogers, David H Owens, Herbert Werner, Chris T Freeman, Paul L Lewin, Stefan Kichhoff, Christian Schmidt, and Gerwald Lichtenberg. Norm optimal iterative learning control with application to problems in accelerator based free electron lasers and rehabilitation robotics. *European Journal of Control*, 16(5):497–524, 2010.

[24] Xiangyu Shao, Guanghui Sun, Weiran Yao, Jianxing Liu, and Ligang Wu. Adaptive sliding mode control for quadrotor UAVs with input saturation. *IEEE/ASME Transactions on Mechatronics*, 27(3):1498–1509, 2021.

[25] Dong Shen. Iterative learning control with incomplete information: A survey. *IEEE/CAA Journal of Automatica Sinica*, 5(5):885–901, 2018.

[26] Zhe Sun, Zhipeng Li, Hao Xie, Yunjun Zheng, Jinchuan Zheng, and Bo Chen. Precise trajectory tracking of mecanum-wheeled omnidirectional mobile robots via a novel fixed-time sliding mode control approach. *Control Theory and Technology*, pages 1–16, 2024. DOI: 10.1007/s11768-024-00224-8.

[27] Abdul Tayebi, S Abdul, MB Zaremba, and Y Ye. Robust iterative learning control design: application to a robot manipulator. *IEEE/ASME Transactions on mechatronics*, 13(5):608–613, 2008.

[28] L. Wang, R. Zhang, and F. Gao. *Iterative learning stabilization and fault-tolerant control for batch processes*. Springer Singapore, 2020.

[29] Ze Wang, Chuxiong Hu, Yu Zhu, Suqin He, Kaiming Yang, and Ming Zhang. Neural network learning adaptive robust control of an industrial linear motor-driven stage with disturbance rejection ability. *IEEE Transactions on Industrial Informatics*, 13(5):2172–2183, 2017.

[30] Qinglai Wei and Derong Liu. Adaptive dynamic programming for optimal tracking control of unknown nonlinear systems with application to coal gasification. *IEEE Transactions on Automation Science and Engineering*, 11(4):1020–1036, 2013.

[31] Xueyan Xing, Sainan Zhang, Tzuhao Huang, Jin Sen Huang, Hao Su, and Yanan Li. Spatial iterative learning torque control of robotic exoskeletons for high accuracy and rapid convergence assistance. *IEEE/ASME Transactions on Mechatronics*, pages 1–13, 2024. DOI: 10.1109/TMECH.2024.3365045.

[32] Wenjun Xiong, Long Xu, Tingwen Huang, Xinghuo Yu, and Yuehao Liu. Finite-iteration tracking of singular coupled systems based on learning control with packet losses. *IEEE Transactions on Systems, Man, and Cybernetics: Systems*, 50(1):245–255, 2017.

[33] Jian-Xin Xu and R. Yan. On initial conditions in iterative learning control. *IEEE Transactions on Automatic Control*, 50(9):1349–1354, 2005.

[34] Shuiqing Xu, Wenzhan Huang, Hai Wang, Weixing Zheng, Juxing Wang, Yi Chai, and Mingyao Ma. A simultaneous diagnosis method for power switch and current sensor faults in grid-connected three-level NPC inverters. *IEEE Transactions on Power Electronics*, 38(1):1104–1118, 2022.

[35] Yu-Tian Xu and Ai-Guo Wu. Integral sliding mode predictive control with disturbance attenuation for discrete-time systems. *IET Control Theory & Applications*, 16(17):1751–1766, 2022.

[36] Xuetao Yang, Hua Wang, and Quanxin Zhu. Event-triggered predictive control of nonlinear stochastic systems with output delay. *Automatica*, 140:110230, 2022.

[37] Xian Yu, Zhongsheng Hou, and Marios M Polycarpou. Distributed data-driven iterative learning consensus tracking for nonlinear discrete-time multiagent systems. *IEEE Transactions on Automatic Control*, 67(7):3670–3677, 2021.

[38] Kun Zhang, Hua-Guang Zhang, Yuliang Cai, and Rong Su. Parallel optimal tracking control schemes for mode-dependent control of coupled markov jump systems via integral RL method. *IEEE Transactions on Automation Science and Engineering*, 17(3):1332–1342, 2019.

[39] Zheshuo Zhang, Bangji Zhang, Dongpu Cao, and Hui Yin. Precise tracking control for articulating crane: Prescribed performance, adaptation, and fuzzy optimality by nash game. *IEEE Transactions on Cybernetics*, 54(1):387–400, 2023.

[40] Quanxin Zhu. Stabilization of stochastic nonlinear delay systems with exogenous disturbances and the event-triggered feedback control. *IEEE Transactions on Automatic Control*, 64(9):3764–3771, 2019.

[41] Zhechen Zhu and Quanxin Zhu. Adaptive fuzzy decentralized control for stochastic nonlinear interconnected system with non-triangular structural dynamic uncertainties. *IEEE Transactions on Fuzzy Systems*, 31(8):2593–2604, 2023.

[]Rongni Yang received the B.S. degree in Mathematics from Shandong University, China in 2006; the M.E. degree and the PhD degree in Control Theory and Control Engineering both from Harbin Institute of Technology, China in 2008 and 2012, respectively. From 2009 to 2011, she was a Research Associate in the Faculty of Advanced Technology, University of South Wales, Pontypridd, U.K. From February 2013 to April 2013, she was a Research Associate in the Department of Mechanical Engineering, The University of Hong Kong. From February 2017 to February 2019, she was a Research Fellow in the School of Computing, Engineering and Mathematics, Western Sydney University, Sydney, Australia. She is currently a Professor in the School of Control Science and Engineering at Shandong University, China. Her current research interests include networked control systems, sliding mode control, iterative learning control and their applications.

Dr. Yang currently serves as an Associate Editor for a number of international journals, including IEEE Transactions on Cybernetics, Circuits, Systems & Signal Processing, and IET Electronics Letters.

[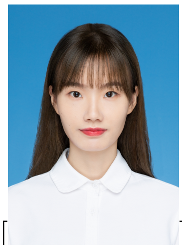]Yingjie Gong received the B.S. degree in Mathematics from Shandong Normal University, China, in 2019 and the M.E. degree in the School of Control Science and Engineering from Shandong University, China, in 2022. She is currently pursuing the Ph.D. degree in control science and engineering at Zhejiang University. Her research interests include iterative learning control, nonlinear control and wind turbine control problems.

[]Wojciech Paszke received the M.Sc. and Ph.D. degrees in electrical engineering from the Technical University of Zielona Góra, in 2000 and 2005, respectively. Between 2008 and 2010 he was affiliated to Eindhoven University of Technology, The Netherlands, where he has been a control systems expert on high precision positioning of electron microscope. Currently, he is affiliated to the Institute of Automation, Electronic and Electrical Engineering at the University of Zielona Góra, Poland. His research interests include multidimensional (nD) systems, repetitive processes, iterative learning control schemes, and convex optimization in robust control problems.